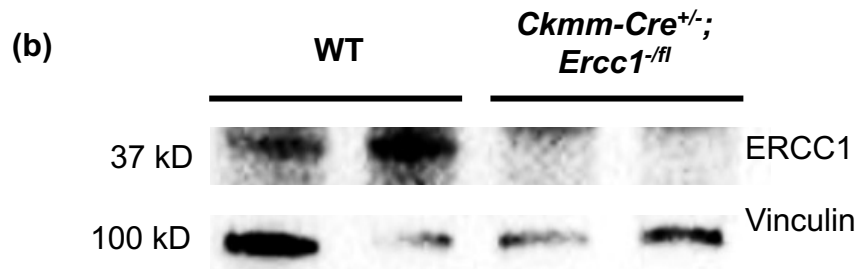
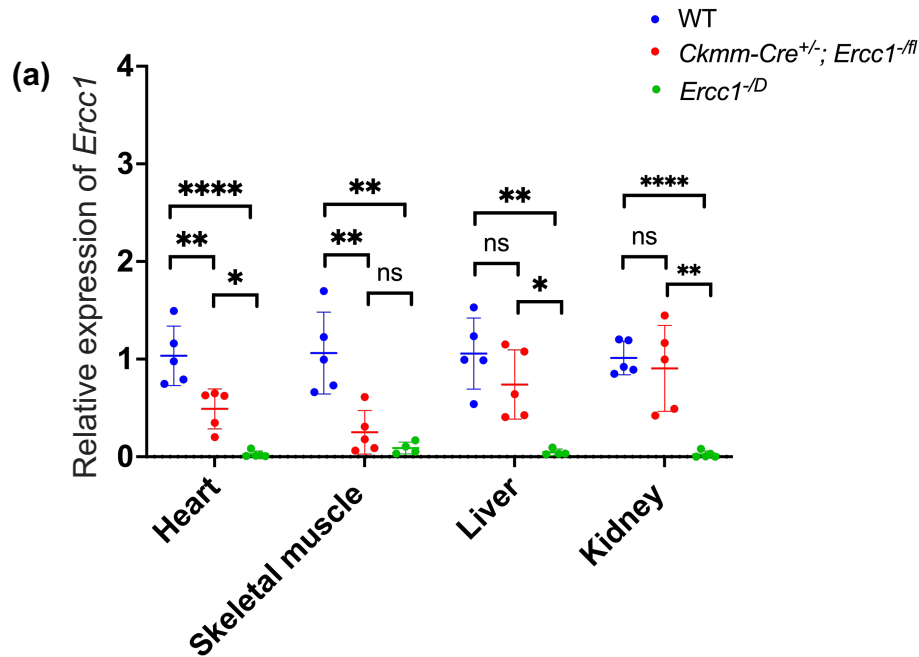
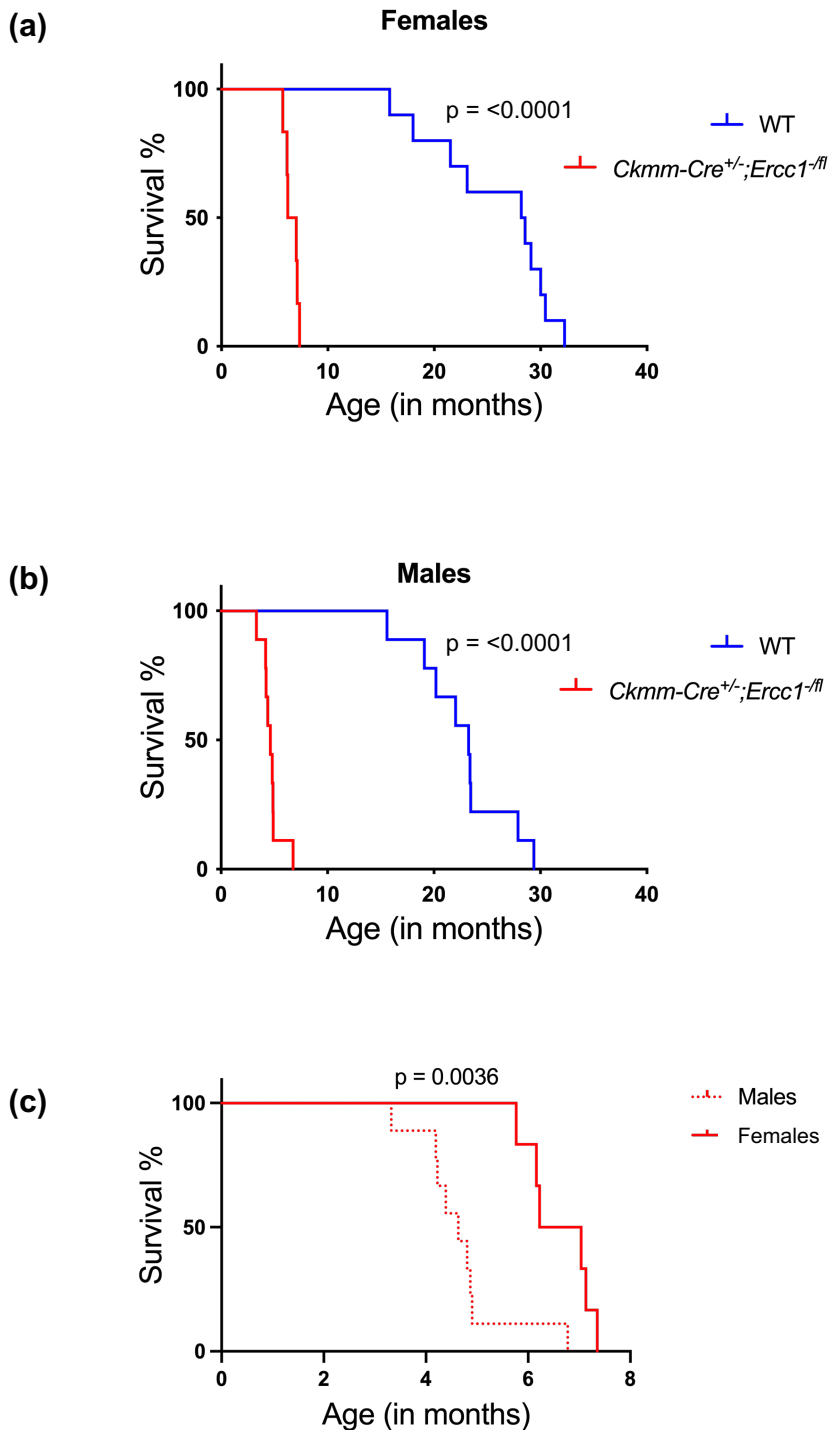


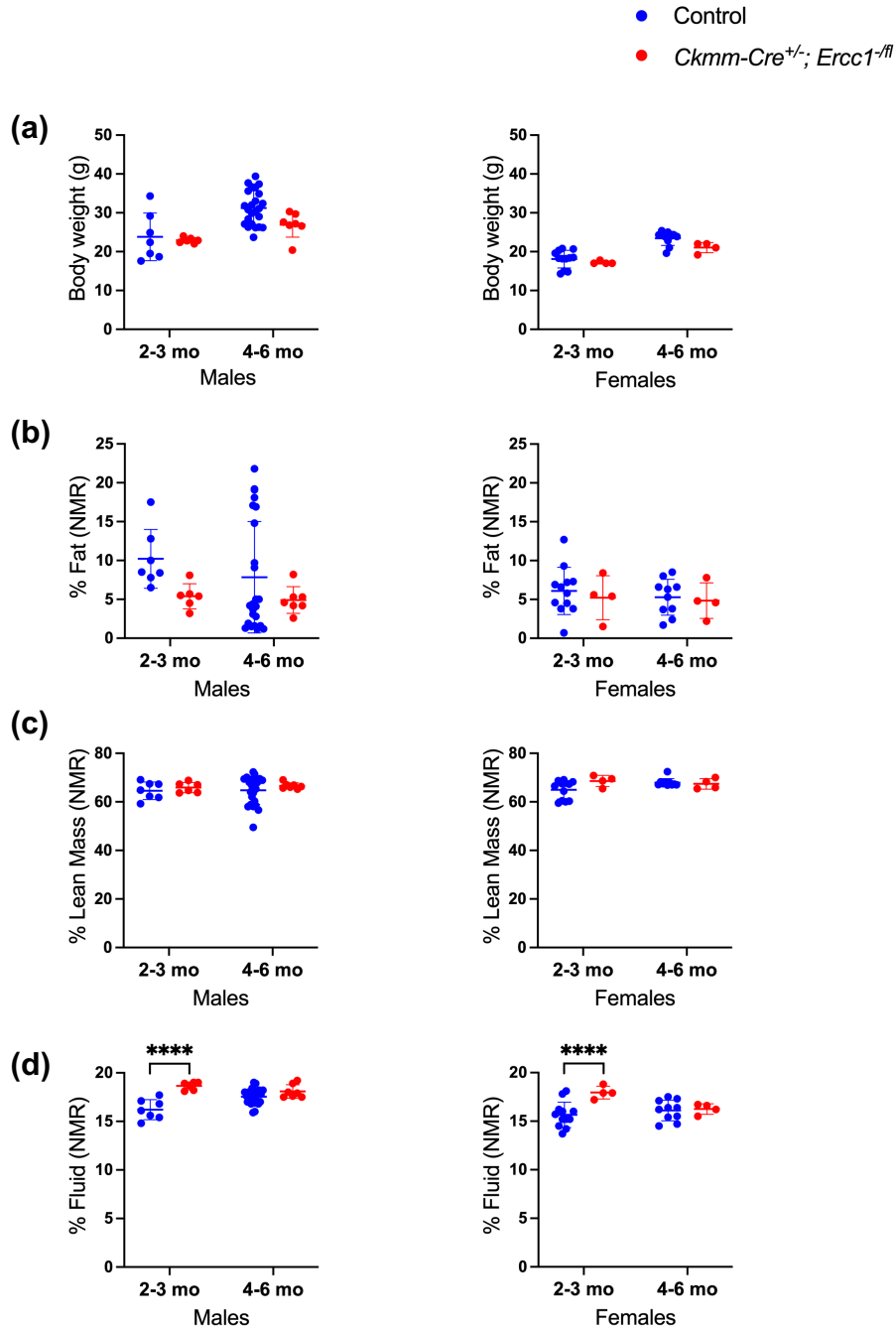
Supplementary Figure 1: Strategy to knock-out *Ercc1* expression in striated muscle of mice. (a). Schematic representation of the wild-type murine *Ercc1* locus, as well as the knock-out, floxed, and recombined alleles. (b). Illustration of breeding scheme for *Ckmm-Cre^{+/-};Ercc1^{-/-}* and (c). *mitCAT;Ckmm-Cre^{+/-};Ercc1^{-/-}* mice. See Supplementary Table 1 for frequency of live births. Figure created using bioRENDER.com (<https://biorender.com/>).



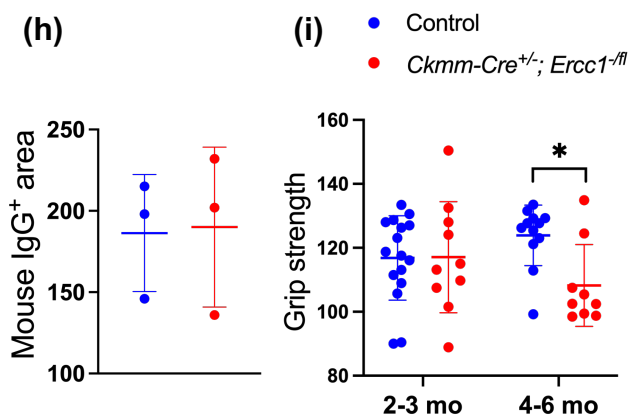
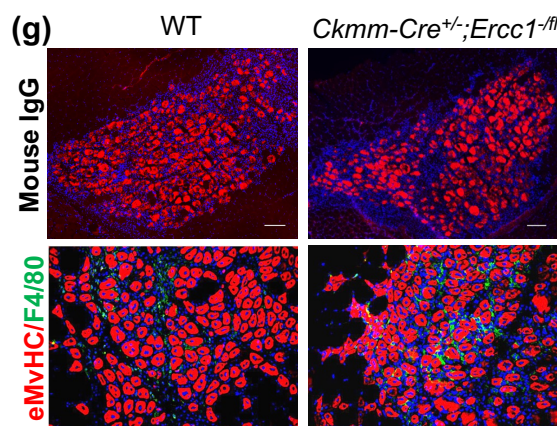
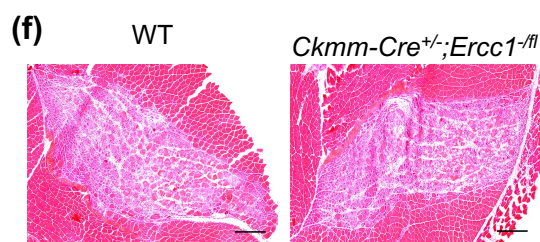
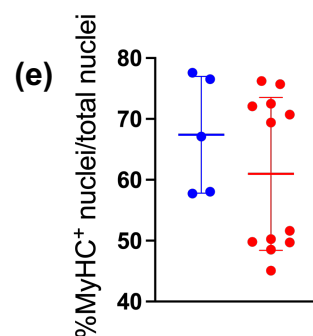
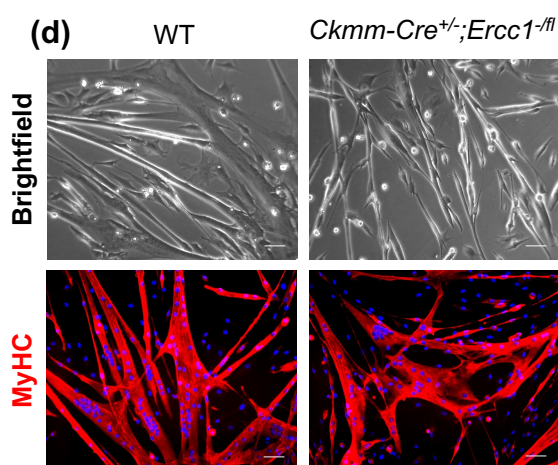
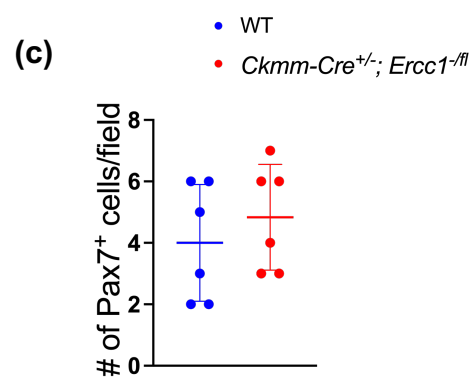
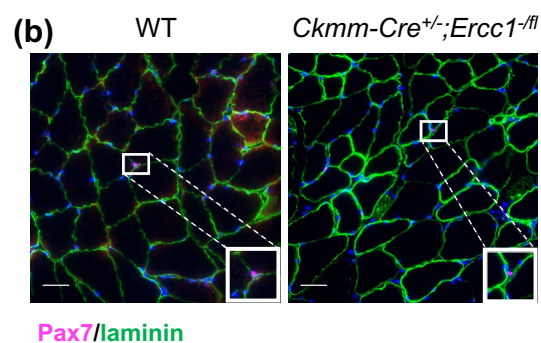
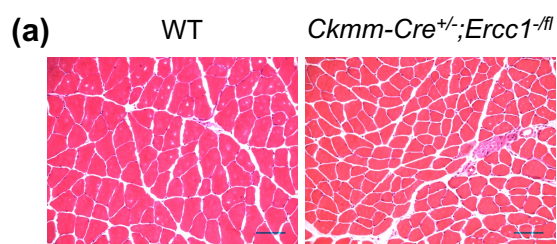
Supplementary Figure 2: *Ercc1* expression in heart, skeletal muscle, liver and kidney from the tissue specific-mutant *Ckmm-Cre*^{+/-}; *Ercc1*^{-fl} mice, *Ercc1*^{-D}, and wild-type (WT) animals. (a). *Ercc1* mRNA levels as measured by qRT-PCR. One-way ANOVA with Tukey's multiple comparison test, * $p < 0.05$, ** $p < 0.01$, **** $p < 0.0001$, and ns = non-significant. See Supplementary Data Table 4 and 5 for primers and the expression of target genes respectively. (b). Immunoblot detection of ERCC1 protein in cardiac tissue of *Ckmm-Cre*^{+/-}; *Ercc1*^{-fl} mice and a littermate WT control. Vinculin was used as a loading control. See Supplementary Data Table 5 for expression of target genes.



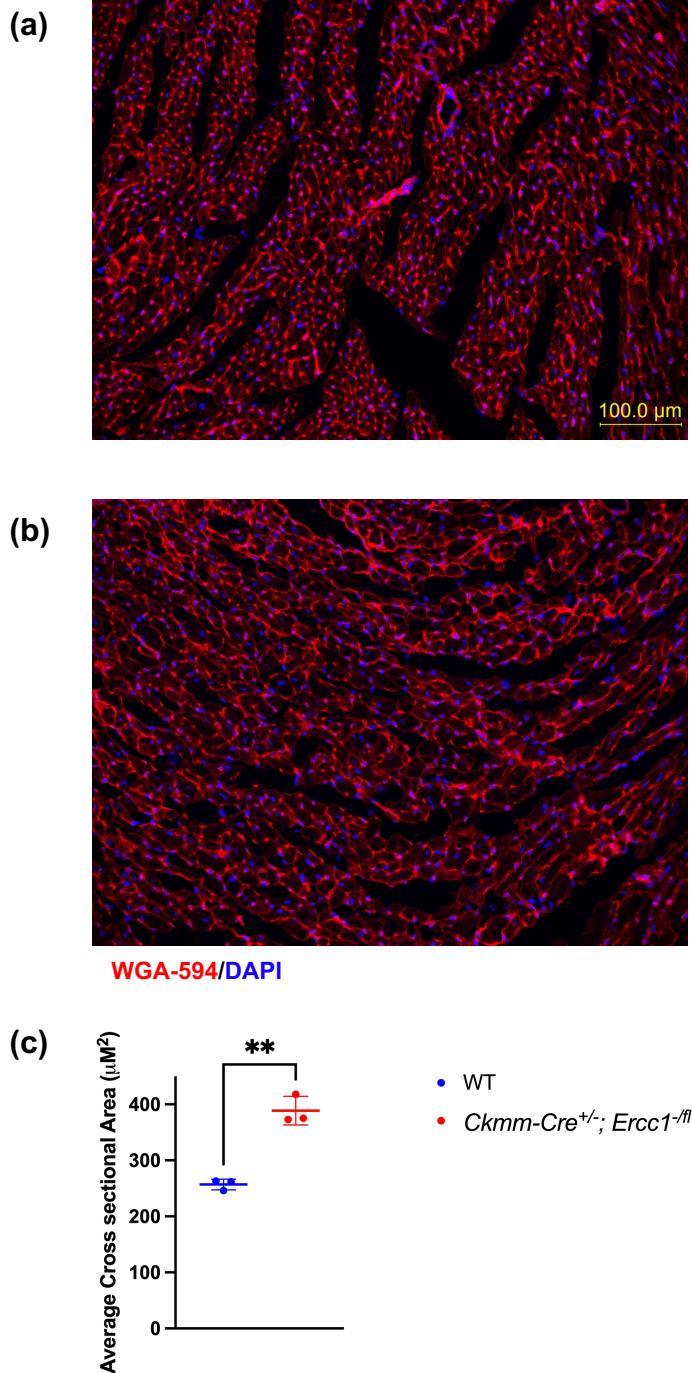
Supplementary Figure 3: Reduced lifespan in both female and male *Ckmm-Cre^{+/-};Ercc1^{-ffl}* mice. Kaplan-Meier survival curves demonstrating that loss of *Ercc1* expression in differentiated myocytes leads to a significantly reduced lifespan of *Ckmm-Cre^{+/-};Ercc1^{-ffl}* mice (a). in females (n=6-10) and (b). males (n=9), $p < 0.0001$, Log-rank (Mantel-Cox) test. (c). Kaplan-Meier survival curves showing that loss of *Ercc1* in differentiated myocytes leads to a significantly reduced lifespan in male mice compared to females.



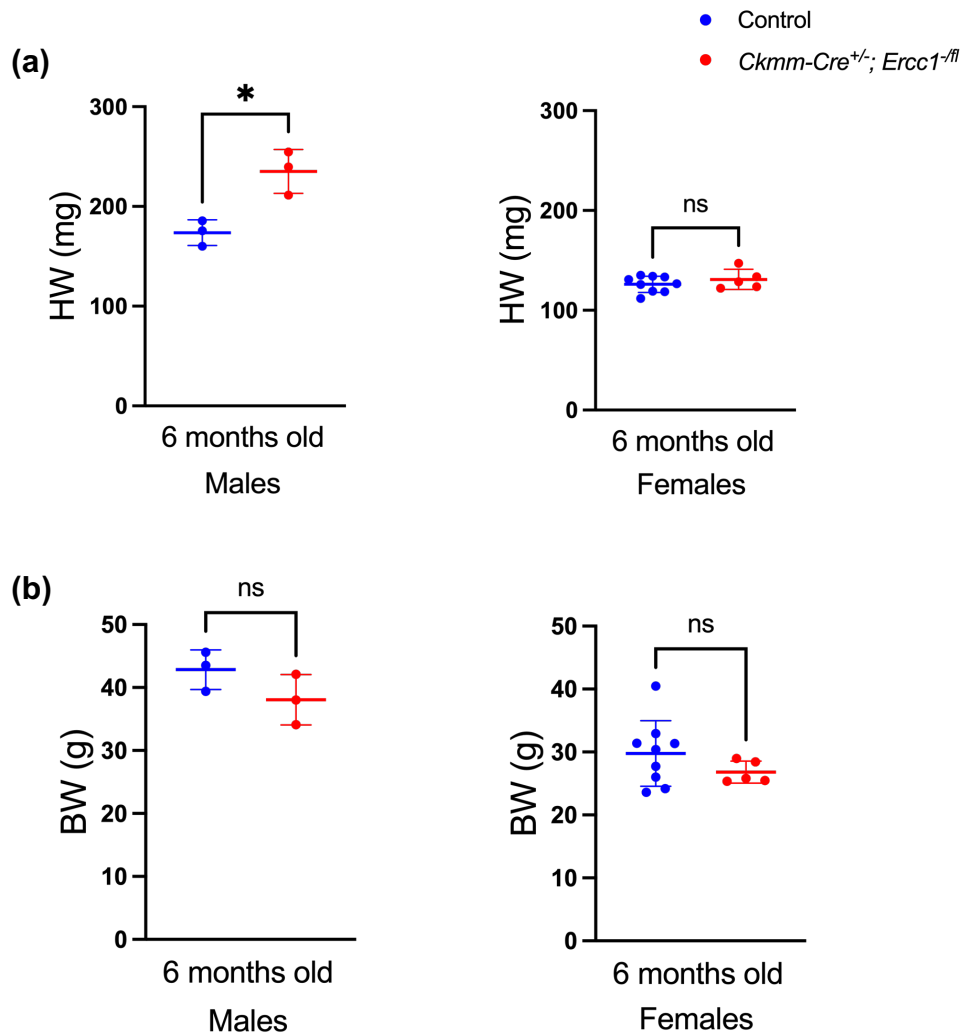
Supplementary Figure 4: Body weight and composition. (a). Weights of male and female mice at two ages. (b-d). Time domain nuclear magnetic resonance (NMR) measure of (b). body fat, (c). lean mass, and (d). fluid of 2-3- and 4-6-month-old male (left) and female (right) mice of *Ckmm-Cre^{+/-}; Ercc1^{-/-}* and WT littermates. Data are represented as the mean \pm SD, n=6-24 per group, One-way ANOVA ****p<0.0001.



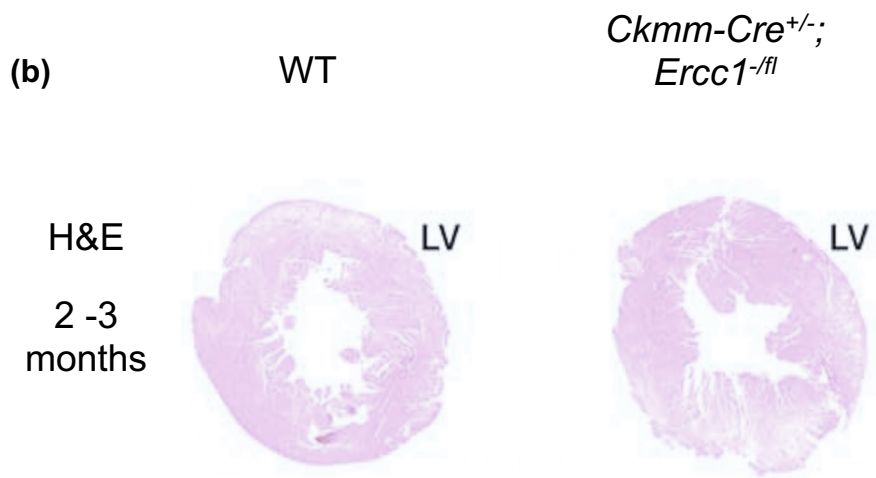
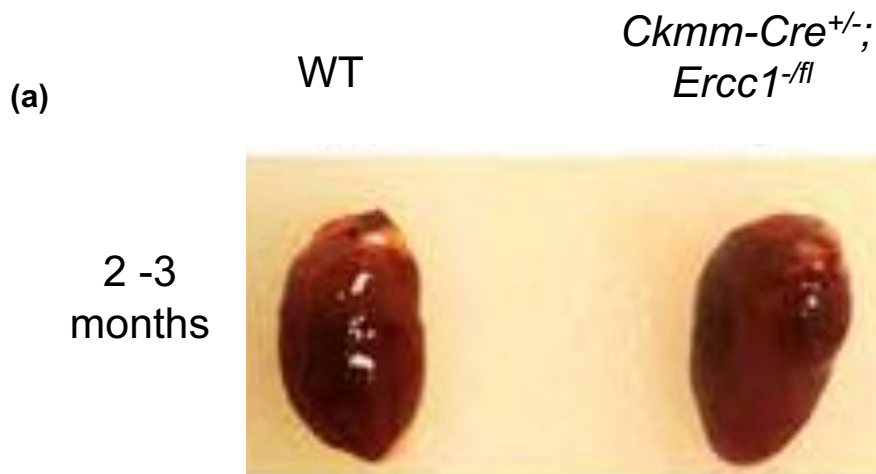
Supplementary Figure 5: Analysis of skeletal muscle in *Ckmm-Cre^{+/-};Ercc1^{-ff}* mice. (a). H&E stained sections of quadriceps from a 6-month-old *Ckmm-Cre^{+/-};Ercc1^{-ff}* mouse and WT littermate showing normal histology as evaluated by light microscopy. Scale bar = 50 μ m. (b). Section of gastrocnemius muscle immunostained for Pax7 (red) to identify satellite cells and laminin (green) to identify the basal lamina, where satellite cells reside. Scale bar = 25 μ m. (c). Quantification of the number of satellite cells at 4-6-months-of-age, relative to WT. Data are represented as mean \pm SD, n=6, Two-tailed, unpaired Student's *t* test, no significant differences found. (d). Representative images of in vitro myogenic differentiation of muscle-derived stem/progenitor cells (MDSPCs) at 4-6 month of age (top). Cells were immunostained for the terminal differentiation marker myosin heavy chain (f-MyHC in red). Scale bar = 50 μ m. Differentiation of MDSPCs isolated from mutant mice was not affected (n=3 cell populations from 3 mice of each genotype), nor was proliferation (data not shown). (e). Quantification of myogenic differentiation (number of nuclei in MyHC⁺ myotubes relative to total number of nuclei). Data represent the mean \pm SD, n=5-6. (f). H&E stained sections of the gastrocnemius muscle to illustrate muscle regeneration 5 days after cardiotoxin injection. Numerous dark staining nuclei in the section illustrate inflammatory infiltration. No difference in muscle regeneration between mutant and WT animals was observed at 4-6 month of age (n=3). Scale bar = 100 μ m. (g). Sections of the regeneration gastrocnemius muscle immunostained for murine IgG to illustrate necrotic fibers (top) or embryonic myosin heavy chain (red) and F4/80 (green) to illustrate new regenerated myofibers and macrophages, respectively. No difference in necrosis, inflammation, or muscle regeneration after injury were observed at 4-6 months (n=3). Scale bar = 100 μ m. (h). Quantitation of mouse IgG after muscle injury. Data are represented as mean \pm SD, n=3. (i). Grip strength of *Ckmm-Cre^{+/-};Ercc1^{-ff}* mice declined modestly in 4-6-month-old mice (Control genotypes[#] n=16; *Ckmm-Cre^{+/-};Ercc1^{-ff}* n=9) mice per age group. Two-tailed Student's *t* test *p<.05. Data represent the mean \pm SD. [#]Control group including WT, *Ercc1^{-ff}*, *Ckmm-Cre^{+/-}* and *Ercc1^{+/-}* mice.



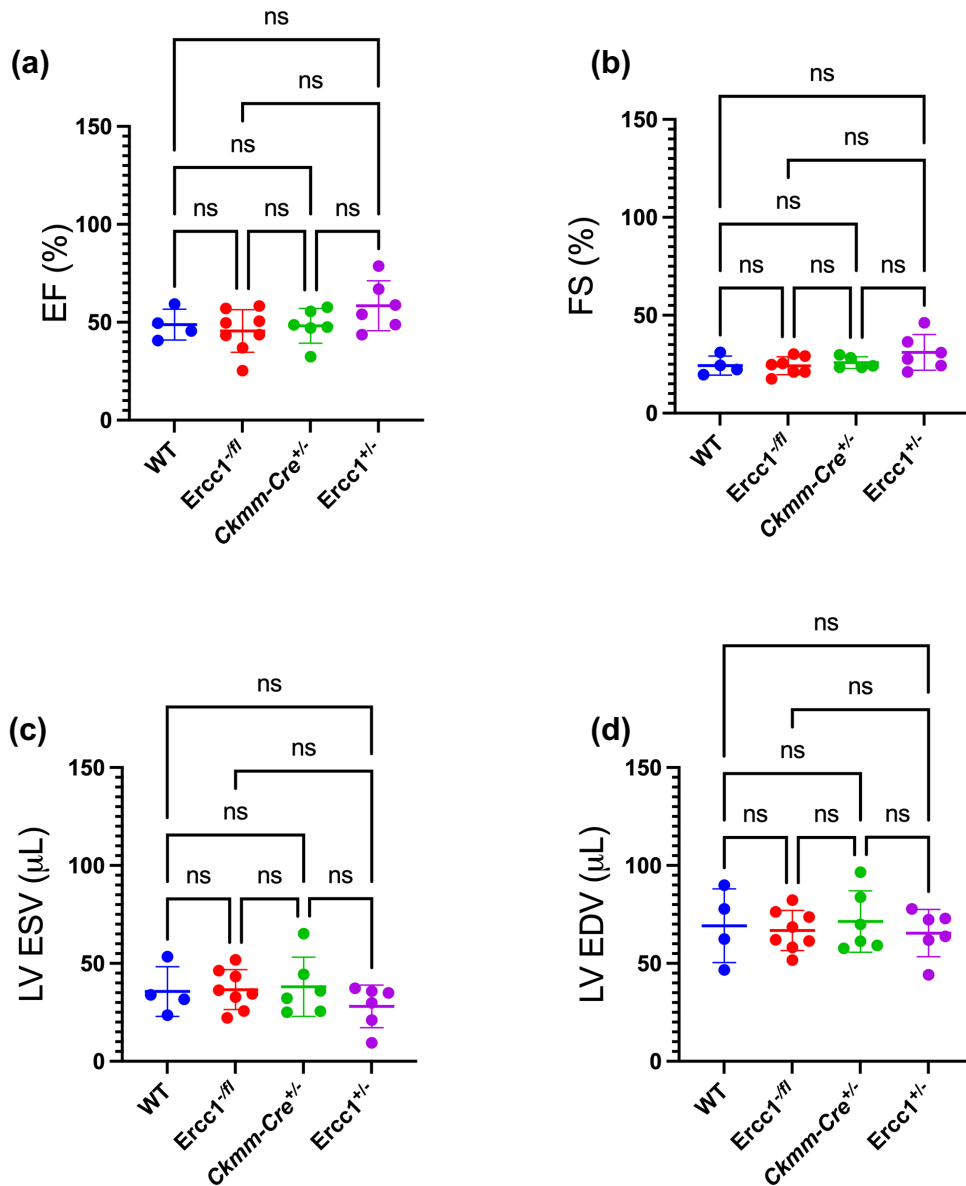
Supplementary Figure 6: Enlarged myocytes of *Ckmm-Cre*^{+/-};*Ercc1*^{-fl}
Representative images of cardiac muscle tissue sections in (a). WT and (b). *Ckmm-Cre*^{+/-};*Ercc1*^{-fl} with WGA-594 staining to detect cell membrane. Sections from 5-month-old WT and *Ckmm-Cre*^{+/-};*Ercc1*^{-fl} mice (n=3). (c). Quantification of myocyte cross-sectional area in cardiac muscle tissue sections in WT and *Ckmm-Cre*^{+/-};*Ercc1*^{-fl} mice. Data represent the mean \pm SD, n=3 per group, 7 technical replicates per animal, Two-tailed, paired Student's *t* test, **p<0.001.



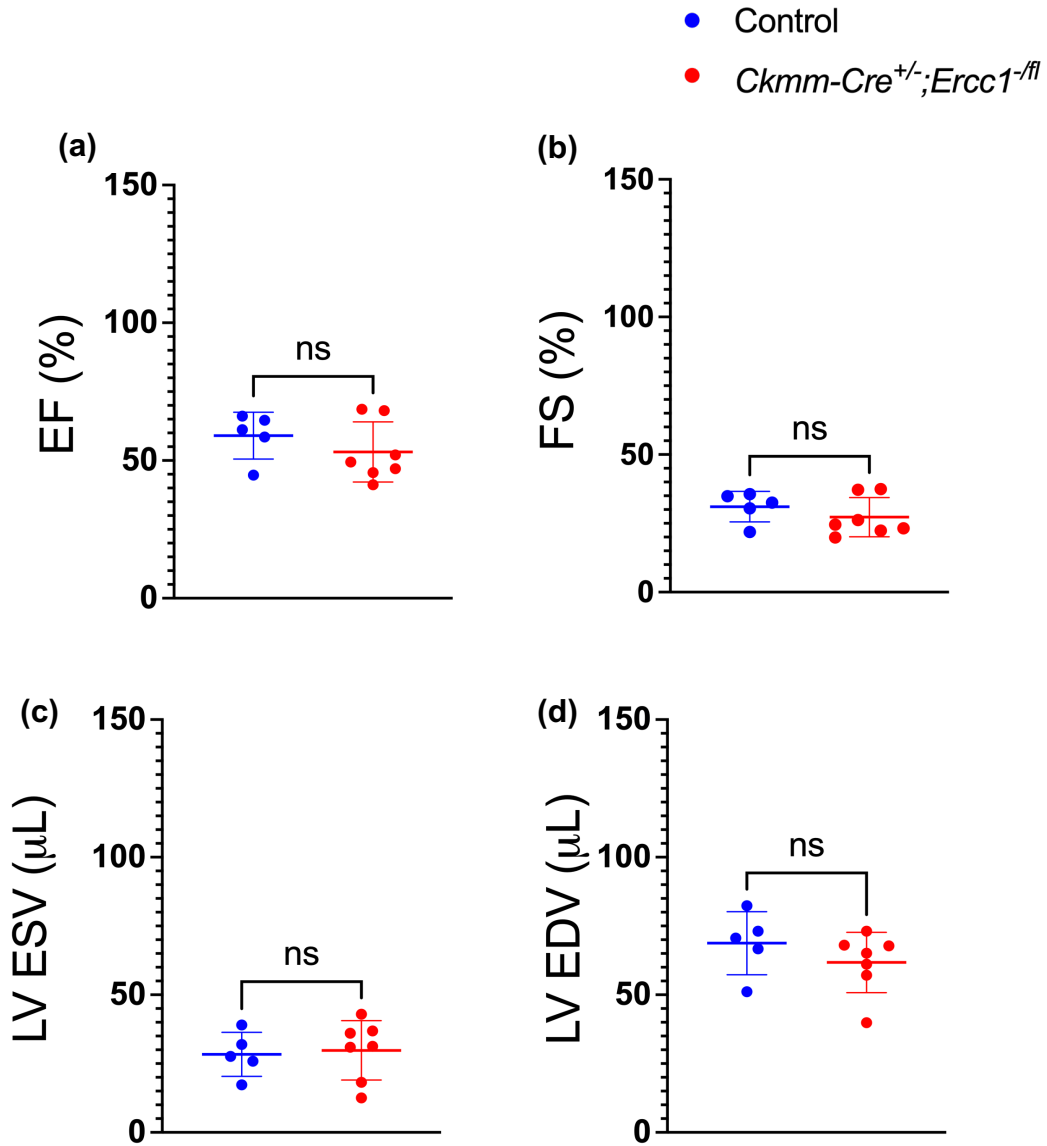
Supplementary Figure 7: Body weight (BW), and heart weight (HW) at 6-months-of-age. (a). Heart weights and (b). Body weight of male and female mice at 6-months-of-age. Data represent the mean \pm SD, $n = 3-9$ mice per group. Two-tailed, unpaired Student's t -test, ns = non-significant.



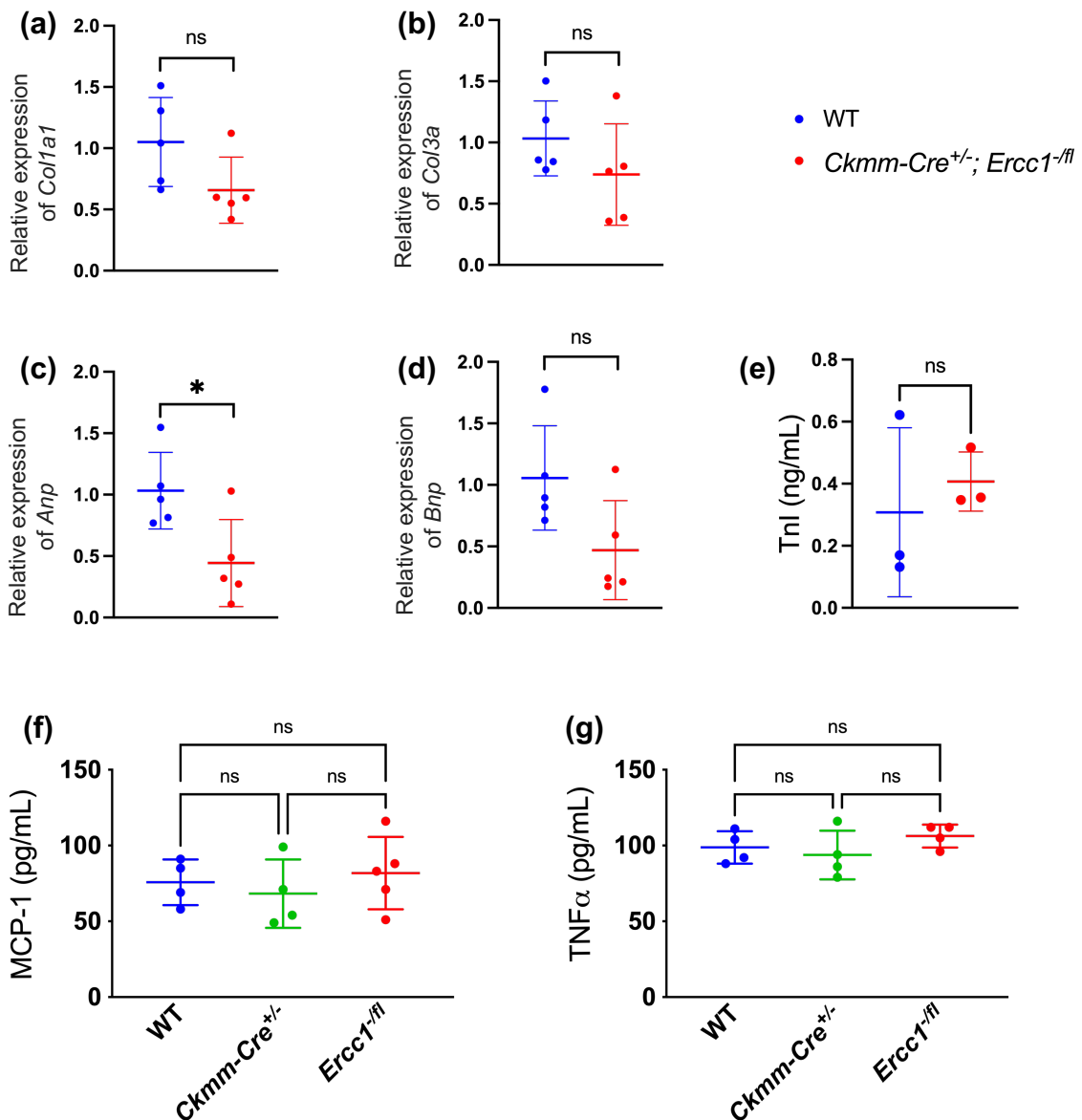
Supplementary Figure 8: Morphologically normal heart in young adult *Ckmm-Cre^{+/-};Ercc1^{-fl}* mice.** (a). Representative images of hearts from a *Ckmm-Cre^{+/-};**Ercc1^{-fl}* mouse and WT littermate at 2-3-months-of-age. (b). Representative images of H&E stained transverse section of the heart from a *Ckmm-Cre^{+/-};**Ercc1^{-fl}* mouse and a WT littermate at 2-3-months-of-age. LV = left ventricle.



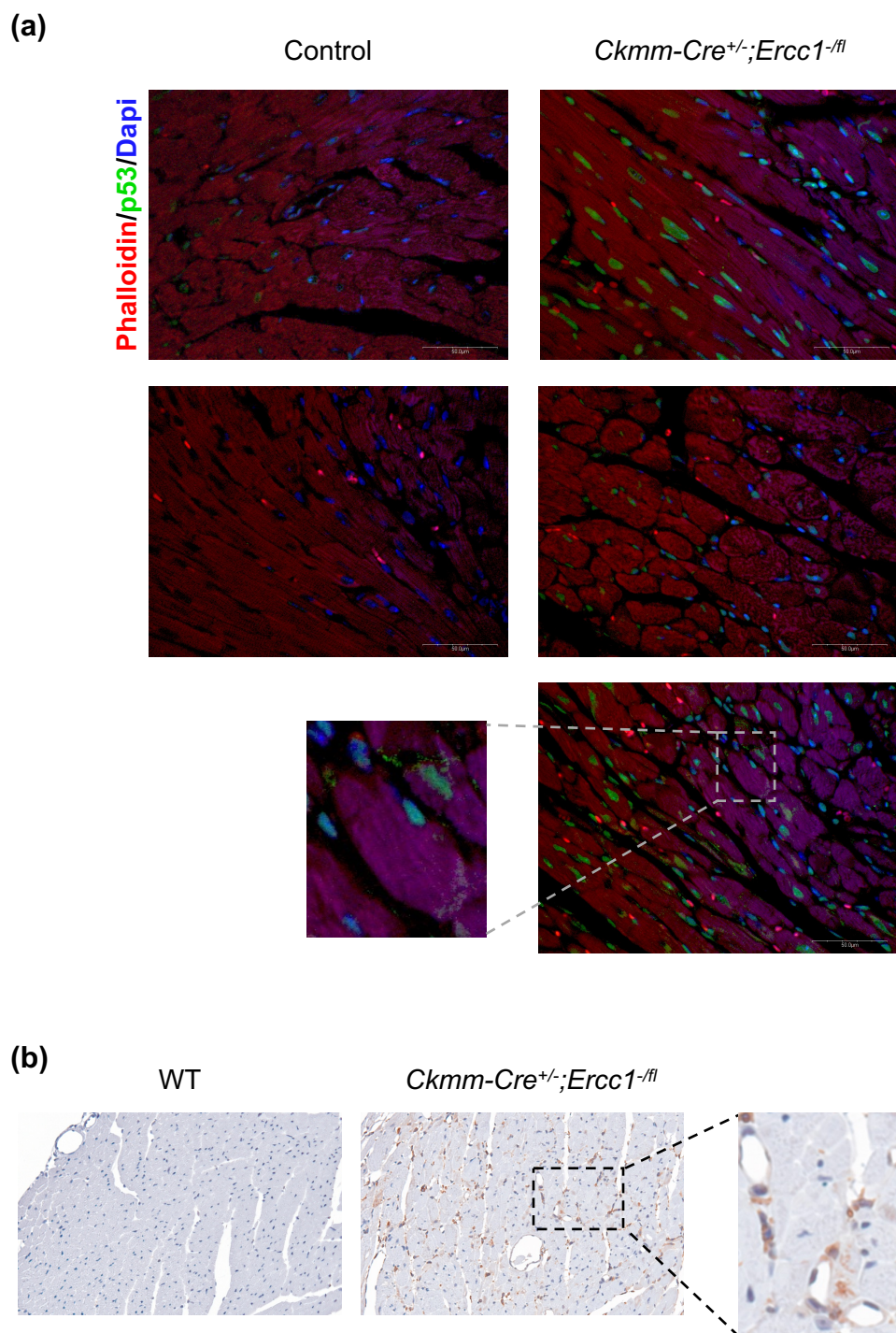
Supplementary Figure 9: Cardiac function in control animals by genotype. Echocardiography data from the control group in main Figure 2 broken out by genotype. (a). Ejection fraction; (b). fractional shortening; (c). left ventricular end systolic volume; (d). left ventricular end diastolic volume. Data represent the mean \pm SD (n=4-8 per group, 6-months-of-age). One-way ANOVA with Tukey's multiple comparison test, ns = non-significant.



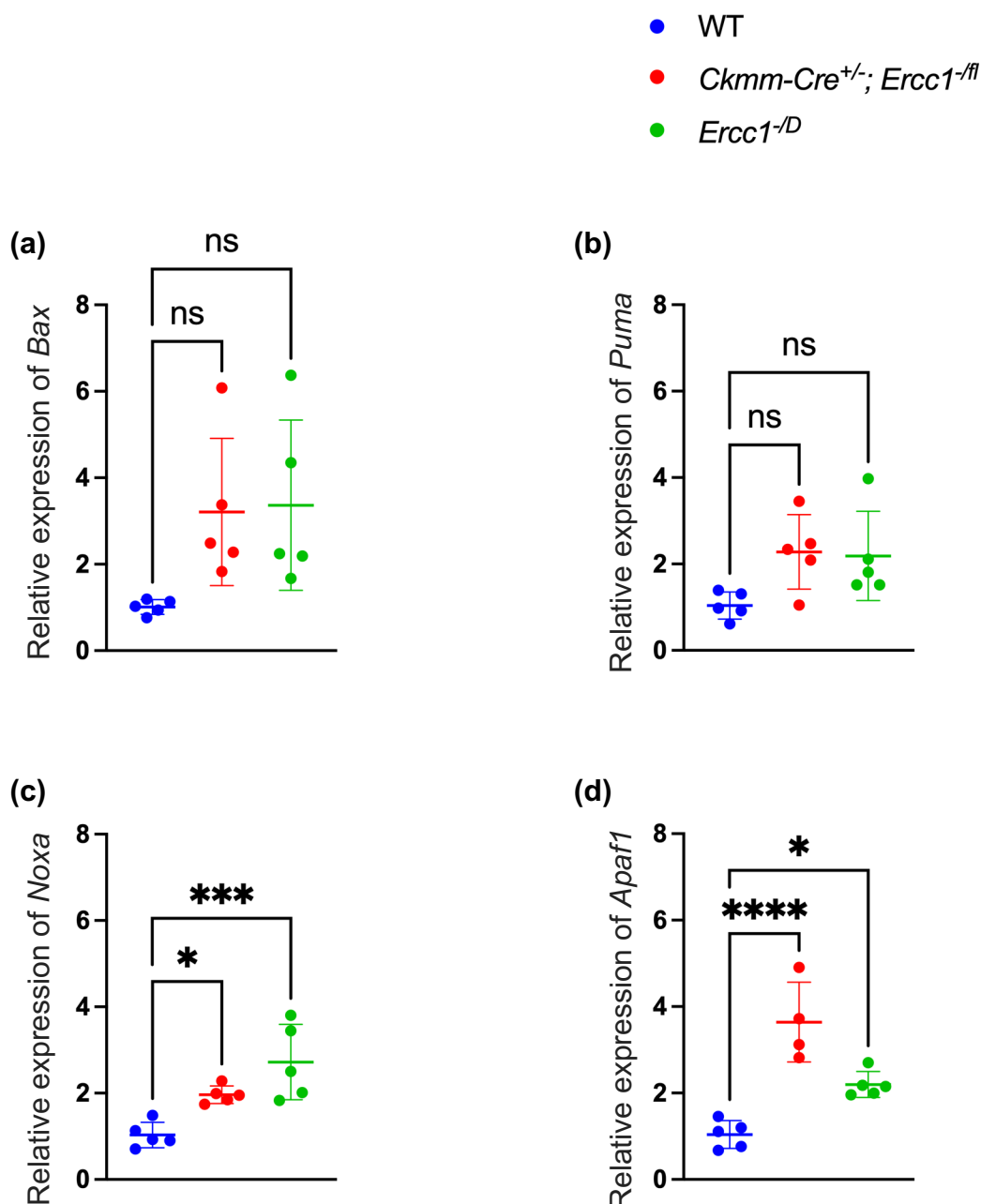
Supplementary Figure 10: Young adult *Ckmm-Cre^{+/-};Ercc1^{-/-}* mice do not have impaired cardiac function. Echocardiography data from 3-4-month-old mutant animals and littermate controls was used to calculate (a). Ejection fraction; (b). fractional shortening; (c). left ventricular end systolic volume; (d). left ventricular end diastolic volume. Data represent the mean \pm SD, n=5-7 per group. Welch's t test (unpaired, two-tailed) ns = non-significant.



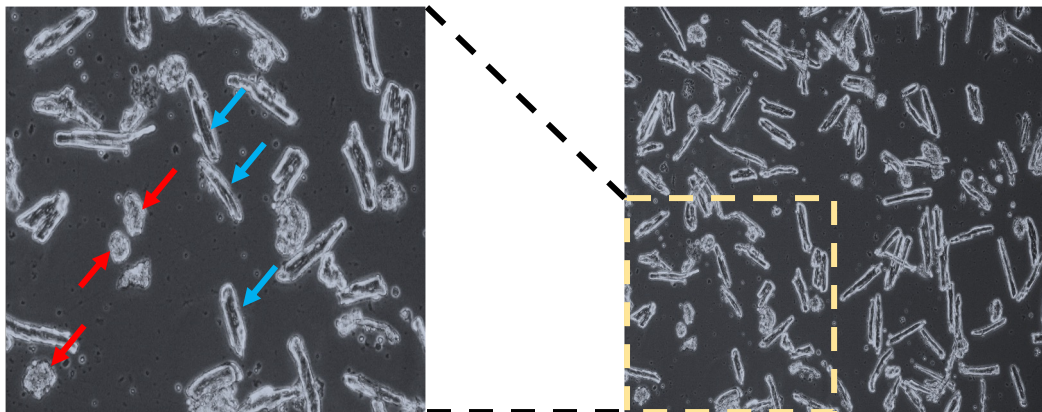
Supplementary Figure 11: Expression of collagen genes and heart failure markers in young adult mice. qRT-PCR measure of the relative expression of the following genes in left ventricular tissue from mutant and WT mice at 2-3 months of age. (a). *Col1a1*; (b). *Col3a*; (c). *Anp*, and (d). *Bnp*, as markers of cardiac fibrosis and failure. Data represent the mean \pm SD, $n=5$ animals per genotype. See Supplementary Data Table 4 and 5 for primers and the expression of target genes respectively. (e). Serum cardiac troponin measured by ELISA. Data represent the mean \pm SD ($n = 3$ mice, 2-3-months of age). Two-tailed, unpaired Student's t test, ns = non-significant. (f-g). Levels of inflammatory markers in serum of control mice by genotype. (f). MCP-1 and (g). Tumor Necrosis Factor- α (TNF- α) in mice of indicated genotypes. Data represent the mean \pm SD ($n=4-5$ per group 2-3-months of age). One-way ANOVA with Tukey's multiple comparison test, ns = non-significant.



Supplementary Figure 12: Elevated levels of p53 in cardiac tissue of *Ckmm-Cre^{+/-};Ercc1^{-fl}* mice. **(a).** Representative fluorescent images of cardiac muscle tissue sections with immunodetection of p53 and staining with phalloidin to detect actin (cardiac myocyte architecture). Sections from 5-month-old control and *Ckmm-Cre^{+/-};Ercc1^{-fl}* mice (n=2, or 3, respectively). **(b).** Immunohistochemistry to detect p53 in cardiac tissue sections from 6-month-old WT and *Ckmm-Cre^{+/-};Ercc1^{-fl}* mice.

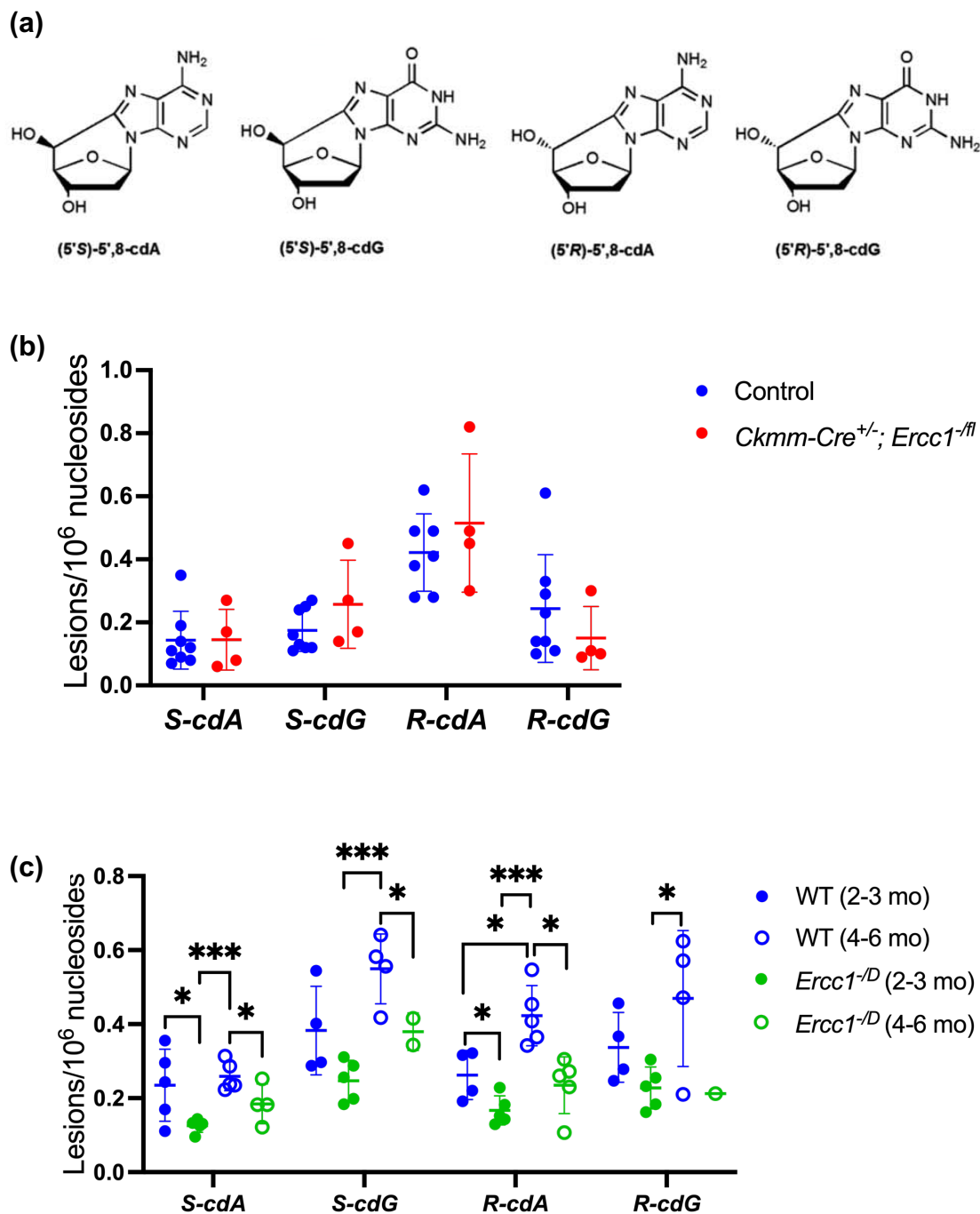


Supplementary Figure 13: Expression of pro-apoptotic p53 target genes in heart tissue of young adult mice. Expression of (a). *Bax*, (b). *Puma*, (c). *Noxa*, and (d). *Apaf1* in cardiac tissues from 2-3-month-old mice of the indicated genotypes measured by qRT-PCR. Graphed is the mean \pm SD. $n=4-5$ animals per genotype. One-way ANOVA was used for statistical analysis, * $p<0.05$; *** $p<0.001$; **** $p<0.0001$ and ns = non-significant. See Supplementary Data Table 4 and 5 for primers and the expression of target genes respectively.

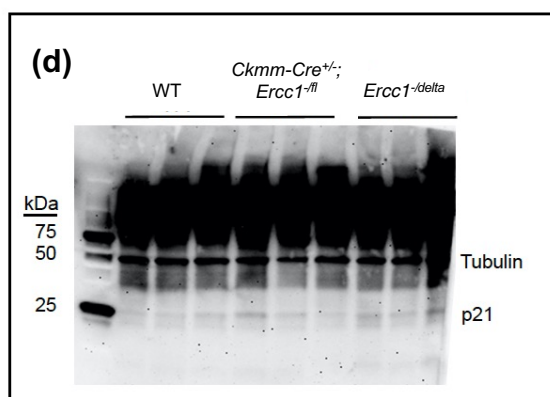
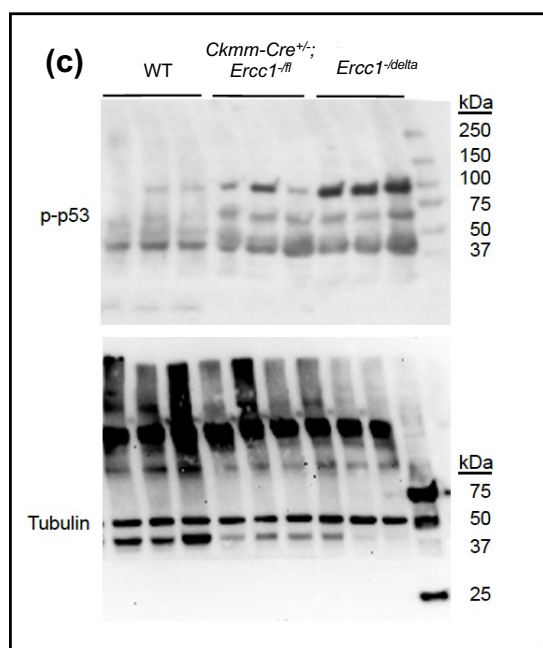
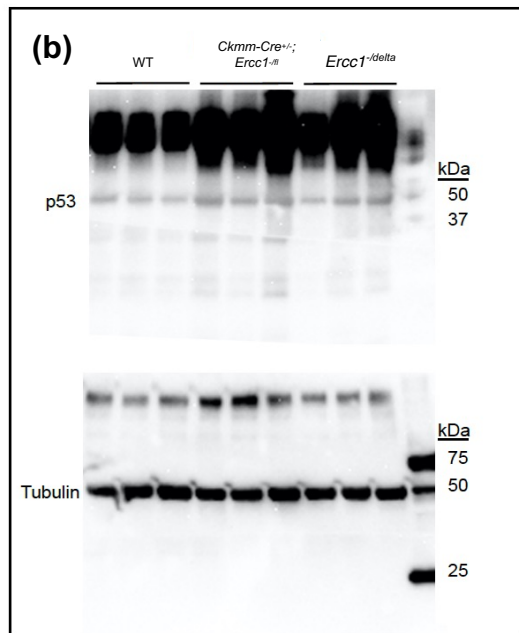
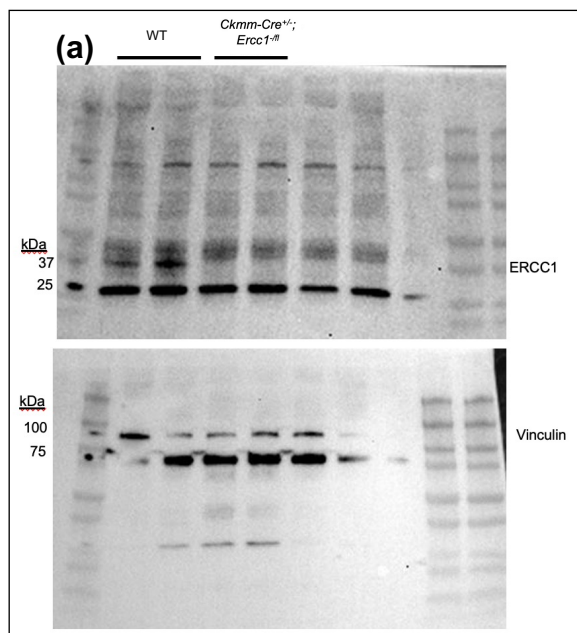


→ Rod (viable)
→ Round (dying)

Supplementary Figure 14: Morphology of viable (rod) and dying (round) cardiac myocytes in vitro.



Supplementary Figure 15: Quantitation of cyclopurine oxidative DNA lesions in cardiac tissue. (a). Structures of the four cyclopurine (cPus) DNA adducts S-cdA, S-cdG, R-cdA and, R-cdG spontaneous oxidative DNA lesions repaired by nucleotide excision repair, an ERCC1-dependent DNA repair mechanism. (b). Quantitation of cPus in cardiac tissue of 4-5-month-old *Ckmm-Cre^{+/-}; Ercc1^{-ffl}* mice and control littermates. Graphed is the mean \pm SD, $n=4-8$ animals per group. All ns by one-tailed, Student's *t* test. (c). Quantitation of cPus in cardiac tissue of 2-3-month-old and 4-6-month-old *Ercc1^{-/-}* and WT mice. Graphed is the mean \pm SD. $n=1-5$ animals per group. One-way ANOVA * $p<0.05$; *** $p<0.001$.



Supplementary Figure 16: Uncropped western blots with marker ladders. (a). Immunoblot detection of ERCC1 protein in tissue lysates from the heart of *Ckmm-Cre^{+/+};Ercc1^{-ff}* mice and a littermate WT controls. Vinculin was used as a loading control. **(b-d).** Immunoblot detection of p21, p53 or (phospho) p-Ser15-p53. Tubulin was used as a loading control.